Intensity comparison between UV lamps and plasma emission for air purification studies

Cite as: AIP Advances 11, 085209 (2021); doi: 10.1063/5.0057033
Submitted: 18 May 2021 • Accepted: 24 July 2021 •
Published Online: 6 August 2021

C. Piferi, A. Brescia, and C. Riccardi[a)]

AFFILIATIONS

Department of Physics, University of Milano-Bicocca, Piazza della Scienza 3, 20126 Milano, Italy

[a)]Author to whom correspondence should be addressed: claudia.riccardi@unimib.it

ABSTRACT

We compared spectra and intensity light of different sources, such as a UV-A lamp, a UV-C lamp, and a visible bulb, and atmospheric nonthermal plasma emission. Spectroscopic measurements were performed with an optical emission spectrometer and radiometric measurements with a radiometer to which UV-A, UV-C, and visible probes were coupled to measure the light intensity per unit surface. For each light source, we measured the emission spectrum and light intensity using different probes and also varying the relative distance. The nonthermal atmospheric plasma was generated by means of a surface barrier dielectric discharge varying the relevant parameters. This work allowed us to create the experimental setup suitable for further studies on volatile organic compound abatement by plasma-catalysis processing and compared it to the photocatalysis techniques based on UV and visible lamps.

I. INTRODUCTION

Nonthermal plasmas are generated in nonthermodynamical equilibrium. They are weakly ionized, containing a few electrons and ions and several atomic and molecular species at high excitation levels. These plasmas are characterized to be composed of high reactive species at ambient temperature and are largely employed for various applications.[1–4]

Nonthermal plasmas can be, for instance, employed for creating a chemical reactive environment in which several processing steps can be performed to treat materials for modifying surface properties[5–10] as well as to treat harmful substances to decompose them.[11–16]

The needs for efficient processes for the abatement of harmful substances, including Volatile Organic Compounds (VOCs) emitted in industrial processes, are really strategic to save our environment.

Some competitive processing aimed to reduce VOC concentrations concerns UV photocatalysis.[17–24] Photocatalysis is the activity occurring when a light source interacts with the surface of semiconductor materials, the so-called photocatalysts. During this process, there must be at least two simultaneous reactions occurring: oxidation from photogenerated holes and reduction from photogenerated electrons.

Photocatalysis can be successfully used in a real environment to decompose pollutants and enhance the quality of the atmospheric air. Usually for a material's environmental applications, metal oxides made of Ti, Zn, Mn, and Cu are suitable to induce the photocatalysis reactions. In this regard, the photocatalysis is more easily induced by UV light or/and visible light.

Nonthermal plasmas, in addition to generating reactive species, produce light. With regard to this, plasmas could be used as light sources instead of UV and visible lamps. It is therefore possible to also induce catalytic processes with plasma light, during plasma gas processing, in the presence of a catalyst. This process is very interesting in the application for the decomposition and the abatement of noxious substances, as demonstrated by the previous literature.[25–27]

We are, therefore, interested to use the plasma as a source of both molecular dissociation by charges and oxidating active species and photocatalysis reactions in the presence of a catalyst deposited in the vicinity of the plasma source.

In developing the plasma–catalytic system, we are first interested in studying and comparing the plasma catalytic activity with that induced by UV and visible light.

This work is aimed to create the experimental setup suitable for the study of VOC abatement by both plasma-catalysis and photocatalysis processes.

To this purpose, this paper presents the experimental setup and a study on the optical proprieties of plasma in comparison with those related to UV and visible lamps.

Here, we present a characterization of the spectra and the power per surface unit for different light sources, such as a UV-A lamp, a UV-C lamp, and a visible LED bulb, and plasma emission presenting the experimental setup. This study permits us to further use the nonthermal atmospheric plasma coupled with photocatalytic medium for the VOC depletion.

This paper is organized as follows: In Sec. II, we describe the experimental setup. In Sec. III, we present results of the experimental campaign, the light sources spectra, and the intensity per surface unit in different conditions. In Sec. IV, we present a final discussion of the results.

II. EXPERIMENTAL SETUP

In our experiment, we used a vacuum cross chamber (20 × 20 cm^2 in length and 10 cm in diameter). The plasma source and the catalytic support are placed in a chamber, while the lamps are placed in front of a quartz window facing the catalytic support outside the chamber. Three of the four openings are closed by vacuum gauges, and the last one is left opened for the first part of the experiment when we study the plasma emission light and the light emitted by the lamps. In the last part of the experiment, we close the last opening by a quartz window to study the light emission lamp abatement from a filter. The same chamber will be also used for the VOC depletion experiments placing the plasma and the catalytic plate inside and the lamp outside.

For the characterization of the light sources, we used optical emission spectroscopy and a radiometric system. As light sources, we used an UV-C lamp (UV Lawtronics centered at 253.7 nm), an UV-A lamp (UV Philips Lighting centered at 370 nm), and a visible LED bulb (GLS Osram at 4000 K). All the lamps are powered by 4 W. During the intensity light measurements, we placed the radiometric probe (or alternatively during the spectra analysis, the optical fiber) at the middle of a semi-closed box aligned with the light source, as shown in Fig. 1. To obscure the ambient light, we covered the device with a blanket. The radiometric probes were placed exactly where we will place the photocatalytic support.

For the characterization of the plasma emission, we placed the plasma source inside the chamber and the probe in front of it (Fig. 2). We used an alumina Surface Dielectric Barrier Discharge (SDBD).[2,28–31]

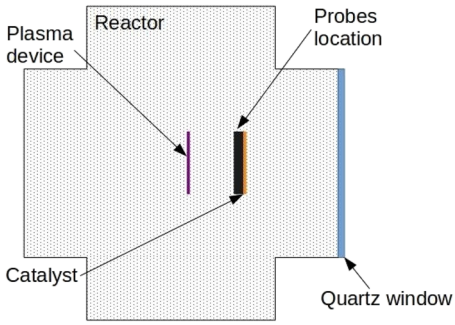

FIG. 2. Plasma device scheme setup.

In our experiment, the SDBD is a 9 × 5 cm^2 alumina dielectric surface, 1 mm thickness, with 9 metal fingers, 7 cm long, 1 mm large, and 4 mm apart made of an alloy of ruthenium, nickel, silver, and palladium. The plasma is lit up by a high voltage (HV) power supply working in a power range between 8 and 80 W and a frequency of the order of tens of kilohertz.[30,31]

A. Optical emission spectroscopy device

The used spectrometer is Ocean Optic PS2000, which works in a range of wavelengths between 180 and 870 nm with a resolution of ~0.3 nm.[1,2] The fiber slit is 10 μm.

B. Radiometric device

As a radiometric device, we used a HD 31 datalogger from DeltaOhm coupled with three radiometric probes that collect the irradiated power per surface unit ($\mu W/cm^2$) in the specified spectra range. The probe are LP47-RAD for visible spectra (400–1050 nm range), LP471-P-A for UV-A spectra (315–400 nm), and LP471-UVC for UV-C spectra (220–280 nm).

Each probe was employed to collect the intensity per surface unit in the specific spectrum range of the light sources.

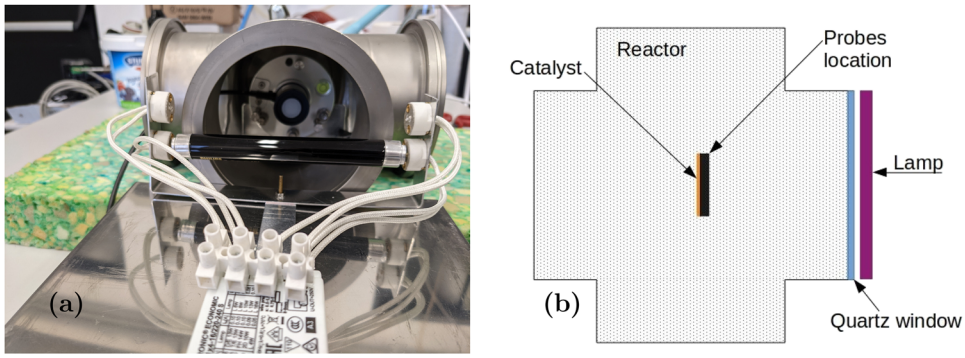

FIG. 1. (a) Lamp equipment setup and (b) scheme.

III. MEASUREMENT RESULTS

For every light source, we measured the optical emission spectra and the radiometric intensity by means of the probes.

A. Optical emission spectroscopy

We used optical emission spectroscopy to characterize the light source spectra (Fig. 3).

The UV-C lamp is characterized by the typical line spectrum of the low pressure Hg: the main peak is at 253.7 nm. The UV-A lamp has only a peak at 370 nm produced by the low pressure Hg vapors, while all the other lines are suppressed by the lamp glass. The visible bulb has a continuous spectrum in the visible range from about 450 to 700 nm. The SDBD plasma is generated at atmospheric pressure in air gas. The plasma emission is characterized by a line spectrum, mainly in the UV-A region, due to the principal, rotational, and vibrational emission of N_2 species. The observed N_2 lines are at 315.93, 337.13, 357.69, 380.49, and 405.94 nm.

We are interested in knowing the light source spectra not only to compare them but also to couple them with the specific catalytic substance for the catalysis processing. Different catalysts are, in fact, activated by different specific light frequencies. In Fig. 3, we can see that plasma emits in the frequency range of the UV-A lamp; in this frequency range, we could expect a synergic effect due to both the light sources in the presence of catalytic support and interactions of the plasma reactive species with the noxious substances. VOC depletion with catalysis activated in the UV-A spectrum region by plasma and UV-A lamp will be the object of future studies.

B. Lamps radiometric measurements

It was observed that the light sources require some time to achieve stable intensity. That time is about 5 min for the UV-A lamp, about 3 min for the UV-C lamp, and about 2 min for the visible bulb.

To set up our apparatus, for each light source, we collected the intensities at different distances between the source itself and the probe, as shown in Fig. 4.

We fitted the UV-A and UV-C data considering the emission source as a uniform limited cylinder (L = 11 cm), so its intensity is

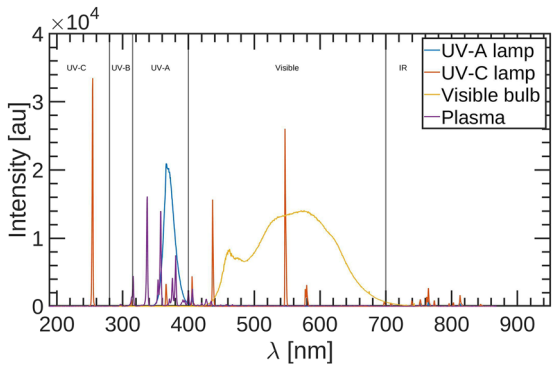

FIG. 3. Spectra emission (in arbitrary units) of the used lamps and plasma detected by the emission spectroscopy device.

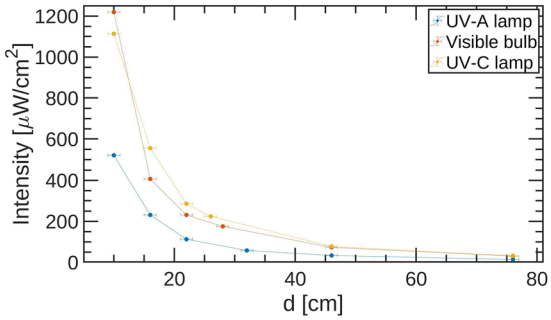

FIG. 4. Intensity (μW/cm^2) vs distance (cm) for the three light sources using the coupled probe.

given by

$$E(d) = 2\frac{A}{d}\left[\text{atan}\left(\frac{L/2}{d}\right)\right] + B, \tag{1}$$

while for the visible bulb, it is a spherical symmetry, and the intensity is given by

$$E(d) = \frac{A}{d^2} + B, \tag{2}$$

where d is the lamp–probe distance.

In Eqs. (1) and (2), the additive parameter B is due to a functional approximation. The errors occurring in the distance measurements are predominant on the intensity ones; to get a better fit, we fitted the inverse function of Eqs. (1) and (2). The fitting curve and parameters are shown in Fig. 5, denoting good agreement between experiments and theory.

Concerning the intensity of the light sources in the other spectrum regions, by radiometric probes, we also found the following:

- Using the UV-A lamp, the visible component is about 0.08 times the UV-A component, while there is no UV-C component.
- Using the UV-C lamp, the visible component is about 0.14 times the UV-C component, while the UV-A component is about 0.02 times the UV-C one.
- Using the visible bulb, there are no UV-A and UV-C components.

We summarize these results in Table I.

Since we are interested in using the catalyst support inside the chamber while the lamps outside the chamber in front of a quartz window, we measured the intensity transmission factor due to the quartz window. The results are shown in Table II. As can be seen, the transmission factor is high and the same in UV-A and visible regions, while it is lower in UV-C light.

C. Plasma radiometric measurements

Using plasma, we measured the intensity per surface unit at different ignition powers at a fixed distance (about 3.5 cm) using both the UV-A and visible probes (Fig. 6). UV-C radiation is almost null in the plasma light.

Comparing the UV-A plasma emission with the UV-A lamp ones at 3.5 cm distance, we found that the latter is between 20

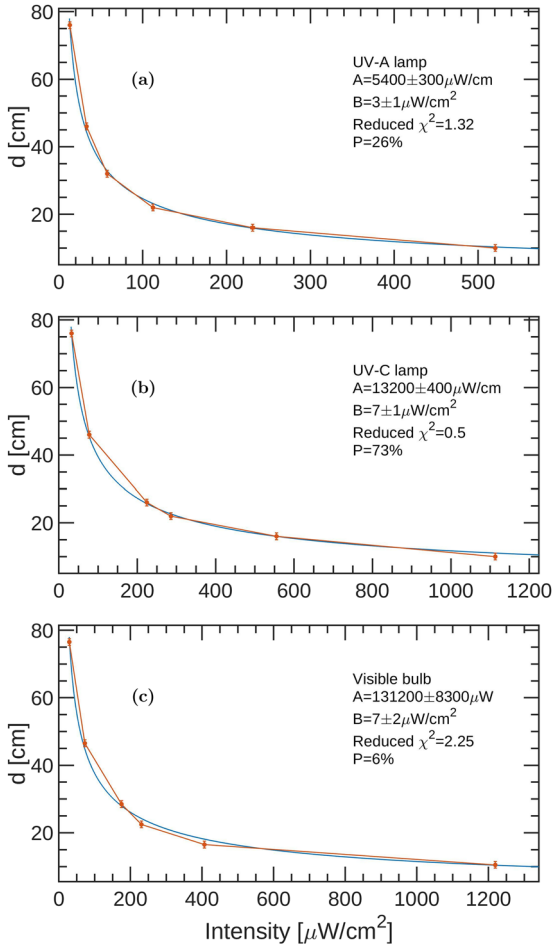

FIG. 5. Fit and experimental data of distance (cm) vs intensity (μW/cm^2) for (a) UV-A, (b) UV-C, and (c) visible light sources.

and 600 times brighter than plasma, depending on their distance from the radiometric probe. A higher intensity factor was found between the visible bulb and the visible component of the plasma.

These results force us to place the catalysts directly on the alumina dielectric surface of our SDBD source between the electrodes. In this way, the catalyst is directly induced by the plasma light, being located at a distance of the order of 1 mm.

TABLE I. Comparison of the intensity emission of the light sources in the different spectrum regions.

Source \ Probe	UV-A	UV-C	Visible
UV-A lamp	1	0	0.08
UV-C lamp	0.02	1	0.14
Visible bulb	0	0	1
Plasma	1	0	0.50

TABLE II. Transmission factor due to the quartz window filter.

Source	Transmission factor (%)
UV-A lamp	80
UV-C lamp	55
Visible bulb	80

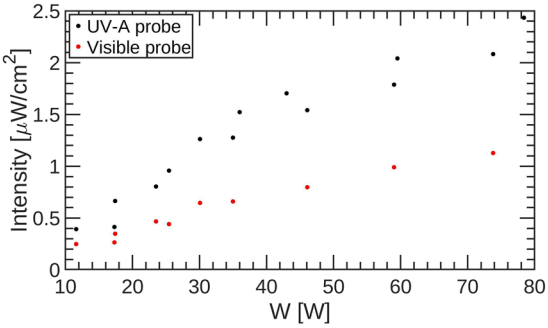

FIG. 6. Intensity (μW/cm^2) vs plasma ignition power (W) for the UV-A probe (black dots) and visible probe (red dots).

IV. DISCUSSION

We investigated the intensity of UV light lamps in comparison with the light emitted by a SDBD plasma at different powers. The intensity of each light source can be summarized in Table I. In this table, we compare the source intensities in the different spectrum regions with respect to the predominant emission spectrum. We demonstrated that the UV-A lamp emits in the UV-A region of the spectrum with also a minor contribution in the UV-C spectrum; the UV-C lamp emits in the UV-C region with a minor contribution in the UV-A spectrum; for the visible LED bulb, it is in the visible region; and for the plasma, the main emission is in the UV-A region.

We also verified that the emission of UV-A and UV-C lamps vs the distance follows Eq. (1), while the visible bulb emission vs the distance follows Eq. (2) and we found the fitting parameters for all our lamps.

Concerning the plasma emission, we found that the intensity is strictly dependent on the applied ignition power and it is much lower than the lamp intensity. This result suggested us to deposit the catalyst near the plasma light, that is, directly on the alumina surface on which plasma is ignited. Then, as the plasma emits both in the visible and in the UV regions, a catalyst can be chosen from among those activated by UV and visible light.

The next step will concern experiments including photocatalysts to study the abatement of various noxious substances. A comparison of photocatalysis processes by lamps and plasma processes with and without the photocatalysts will be object of future studies.[28,29]

ACKNOWLEDGMENTS

We kindly acknowledge the Fondazione di Comunità Milano—Fondo Solidale Professor Ignazio Renato Bellobono

(Grant No. 2020-CONT-0206) for funding our research. We also gratefully acknowledge the technical support of Alessandro Mietner and Alessandro Baù in the device development and experiment execution.

DATA AVAILABILITY

The data that support the findings of this study are available from the corresponding author upon reasonable request.

REFERENCES

[1]I. Biganzoli, R. Barni, and C. Riccardi, "Temporal evolution of a surface dielectric barrier discharge for different groups of plasma microdischarges," J. Phys. D: Appl. Phys. **46**, 025201 (2012).
[2]I. Biganzoli, R. Barni, C. Riccardi, A. Gurioli, and R. Pertile, "Optical and electrical characterization of a surface dielectric barrier discharge plasma actuator," Plasma Sources Sci. Technol. **22**, 025009 (2013).
[3]R. A. Siliprandi, H. E. Roman, R. Barni, and C. Riccardi, "Characterization of the streamer regime in dielectric barrier discharges," J. Appl. Phys. **104**, 063309 (2008).
[4]A. Raffaele-Addamo, C. Riccardi, E. Selli, R. Barni, M. Piselli, G. Poletti, F. Orsini, B. Marcandalli, M. R. Massafra, and L. Meda, "Characterization of plasma processing for polymers," Surf. Coat. Technol. **174–175**, 886–890 (2003).
[5]S. Zanini, A. Citterio, G. Leonardi, and C. Riccardi, "Characterization of atmospheric pressure plasma treated wool/cashmere textiles: Treatment in nitrogen," Appl. Surf. Sci. **427**, 90–96 (2018).
[6]S. Zanini, S. Freti, A. Citterio, and C. Riccardi, "Characterization of hydro- and oleo-repellent pure cashmere and wool/nylon textiles obtained by atmospheric pressure plasma pre-treatment and coating with a fluorocarbon resin," Surf. Coat. Technol. **292**, 155–160 (2016).
[7]S. Zanini, E. Grimoldi, A. Citterio, and C. Riccardi, "Characterization of atmospheric pressure plasma treated pure cashmere and wool/cashmere textiles: Treatment in air/water vapor mixture," Appl. Surf. Sci. **349**, 235–240 (2015).
[8]S. Zanini, C. Riccardi, C. Canevali, M. Orlandi, L. Zoia, and E.-L. Tolppa, "Modifications of lignocellulosic fibers by Ar plasma treatments in comparison with biological treatments," Surf. Coat. Technol. **200**, 556–560 (2005).
[9]R. A. Siliprandi, S. Zanini, E. Grimoldi, F. S. Fumagalli, R. Barni, and C. Riccardi, "Atmospheric pressure plasma discharge for polysiloxane thin films deposition and comparison with low pressure process," Plasma Chem. Plasma Process. **31**, 353–372 (2011).
[10]B. Marcandalli and C. Riccardi, "Plasma treatments of fibres and textiles" in *Plasma Technologies for Textiles*, edited by R. Shishoo (Woodhead Publishing Ltd., 2007), pp. 282–300.
[11]R. Barni, E. Dell'Orto, and C. Riccardi, "Chemical kinetics of the plasma gas-hase in humid air non-thermal atmospheric pressure discharges," Int. J. Plasma Environ. Sci. Technol. **12**, 109–113 (2019).
[12]R. Barni, R. Benocci, N. Spinicchia, H. E. Roman, and C. Riccardi, "An experimental study of plasma cracking of methane using DBDs aimed at hydrogen production," Plasma Chem. Plasma Process. **39**, 241–258 (2019).
[13]S. Zanini, P. Massini, M. Mietta, E. Grimoldi, and C. Riccardi, "Plasma treatments of PET meshes for fuel–water separation applications," J. Colloid Interface Sci. **322**, 566–571 (2008).
[14]R. Barni, P. Esena, and C. Riccardi, "Chemical kinetics simulation for atmospheric pressure air plasmas in a streamer regime," J. Appl. Phys. **97**, 073301 (2005).
[15]R. Barni, I. Biganzoli, E. C. Dell'Orto, and C. Riccardi, "Effect of duty-cycles on the air plasma gas-phase of dielectric barrier discharges," J. Appl. Phys. **118**, 143301 (2015).
[16]R. Barni and C. Riccardi, "Gas-phase evolution of Ar/H_2O and Ar/CH_4 dielectric barrier discharge plasmas," Eur. Phys. J. D **72**, 62 (2018).
[17]A. L. Linsebigler, G. Lu, and J. T. Yates, Jr., "Photocatalysis on TiO_2 surfaces: Principles, mechanisms, and selected results," Chem. Rev. **95**, 735–758 (1995).
[18]P. Di Lazzaro, D. Murra, G. Felici, and S. Fu, "Spatial distribution of the light emitted by an excimer lamp used for ultraviolet-B photo-therapy: Experiment and modeling," Rev. Sci. Instrum. **75**, 1332–1336 (2004).
[19]D. L. Maurer and J. A. Koziel, "On-farm pilot-scale testing of black ultraviolet light and photocatalytic coating for mitigation of odor, odorous VOCs, and greenhouse gases," Chemosphere **221**, 778–784 (2019).
[20]M. Stucchi, F. Galli, C. L. Bianchi, C. Pirola, D. C. Boffito, F. Biasioli, and V. Capucci, "Simultaneous photodegradation of VOC mixture by TiO_2 powders," Chemosphere **193**, 198–206 (2018).
[21]H. Zheng, J. Z. Ou, M. S. Strano, R. B. Kaner, A. Mitchell, and K. Kalantar-zadeh, "Nanostructured tungsten oxide–properties, synthesis, and applications," Adv. Funct. Mater. **21**, 2175–2196 (2011).
[22]H. Xu, S. Ouyang, L. Liu, P. Reunchan, N. Umezawa, and J. Ye, "Recent advances in TiO_2-based photocatalysis," J. Mater. Chem. A **2**, 12642–12661 (2014).
[23]X. Yang, J. A. Koziel, Y. Laor, W. Zhu, J. van Leeuwen, W. S. Jenks, S. J. Hoff, J. Zimmerman, S. Zhang, U. Ravid *et al.*, "VOC removal from manure gaseous emissions with UV photolysis and UV-TiO_2 photocatalysis," Catalysts **10**, 607 (2020).
[24]I. R. Bellobono, F. Groppi, M. Sturini, A. Albini, and F. Morazzoni, "A kinetic approach to photomineralization of methane in air by membranes based on TiO_2/WO_3," J. Chem. Chem. Eng. **14**, 73–85 (2020).
[25]J. Karuppiah, E. L. Reddy, P. Manoj Kumar Reddy, B. Ramaraju, R. Karvembu, and C. Subrahmanyam, "Abatement of mixture of volatile organic compounds (VOCs) in a catalytic non-thermal plasma reactor," J. Hazard. Mater. **237–238**, 283–289 (2012).
[26]L. Sivachandiran, F. Thévenet, and A. Rousseau, "Isopropanol removal using Mn_xO_y packed bed non-thermal plasma reactor: Comparison between continuous treatment and sequential sorption/regeneration," Chem. Eng. J. **270**, 327–335 (2015).
[27]X. Zhu, X. Gao, X. Yu, C. Zheng, and X. Tu, "Catalyst screening for acetone removal in a single-stage plasma-catalysis system," Catal. Today **256**, 108–114 (2015).
[28]I. Biganzoli, R. Barni, and C. Riccardi, "Note: On the use of Rogowski coils as current probes for atmospheric pressure dielectric barrier discharges," Rev. Sci. Instrum. **84**, 016101 (2013).
[29]I. Biganzoli, R. Barni, A. Gurioli, R. Pertile, and C. Riccardi, "Experimental investigation of Lissajous figure shapes in planar and surface dielectric barrier discharges," J. Phys.: Conf. Ser. **550**, 012039 (2014).
[30]P. Esena, S. Zanini, and C. Riccardi, "Plasma processing for surface optical modifications of pet films," Vacuum **82**, 232–235 (2007).
[31]C. Piferi, R. Barni, H. E. Roman, and C. Riccardi, "Current filaments in asymmetric surface dielectric barrier discharge," Appl. Sci. **11**, 2079 (2021).